



Substituted indolin-2-ones as p90 ribosomal S6 protein kinase 2 (RSK2) inhibitors: Molecular docking simulation and structure–activity relationship analysis

Ye Zhong[†], Mengzhu Xue[†], Xue Zhao[†], Jun Yuan, Xiaofeng Liu, Jin Huang, Zhenjiang Zhao^{*}, Honglin Li^{*}, Yufang Xu^{*}

Shanghai Key Laboratory of New Drug Design, State Key Laboratory of Bioreactor Engineering, School of Pharmacy, East China University of Science and Technology, Shanghai 200237, China

ARTICLE INFO

Article history:

Received 13 December 2012

Revised 21 January 2013

Accepted 23 January 2013

Available online 30 January 2013

Keywords:

RSK2

Kinase inhibitor

Molecular docking

ABSTRACT

A series of novel indolin-2-ones inhibitors against p90 ribosomal S6 protein kinase 2 (RSK2) were designed and synthesized and their structure–activity relationship (SAR) was studied. The most potent inhibitor, compound **3s**, exhibited potent inhibition against RSK2 with an IC₅₀ value of 0.5 μM and presented a satisfactory selectivity against 23 kinases. The interactions of these inhibitors with RSK2 were investigated based on the proposed binding poses with molecular docking simulation. Four compounds and six compounds exhibited moderate anti-proliferation activities against PC 3 cells and MCF-7 cells, respectively.

© 2013 Elsevier Ltd. All rights reserved.

1. Introduction

The 90 kDa ribosomal S6 kinase 2 (RSK2) is a serine/threonine kinase and belongs to the RSKs family, which possesses an N-terminal kinase domain (NTKD) and a C-terminal kinase domain (CTKD) connected by a linker region.^{1–9} Presently, RSK2 has been verified to be a promising cancer therapeutic target due to its principal performances in the regulation of diverse cellular process, such as cell transformation, proliferation and invasion.³ Moreover, overexpression of RSK2 is related to many human diseases including breast cancer, prostate cancer, and some hematopoietic stem cell carcinoma.¹⁰ These studies indicate the significance of developing novel and potent RSK2 inhibitors.

To date, dozens of potent RSK2 inhibitors have been reported (Fig. 1). Among them, SL0101 is the first reported specific inhibitor of RSK2, which was extracted from the tropical plant *Forsteronia refracta* and showed an IC₅₀ value of 89 nM.^{11–13} Some classical protein kinase inhibitors are also found to be active but nonspecific against RSK2, such as PKC inhibitors GF109203X and Ro31–8220 obtained from kinase screenings,¹⁴ which may provide useful information to develop RSK2 inhibitors as well.^{15–17} Moreover, Fmk is an inhibitor designed to irreversibly bind to the CTKD of

RSK2 and exhibits potent inhibition with an IC₅₀ of 15 nM.¹⁸ However, only two crystal structures of RSK2 NTKD complexed with similar inhibitors have been released recently,¹⁹ representing one determinate binding mode of such inhibitors, but none of them are used in the clinical trials. Therefore, there are growing needs for developing more potent RSK2 inhibitors to ensure their clinical applicability.

Using the ligand-based virtual screening program SHAFTS and structure-based virtual screening protocols, our group discovered a variety of compounds with potent or moderate inhibitory activities against RSK2, most of which have novel scaffolds different from the reported RSK2 inhibitors.^{20–23} Among them, compounds with an indolin-2-ones scaffold inspired us to perform structural screening to improve the inhibitory activity and some of them were reported as inhibitors against other kinases.^{24–27} In this study, the designed novel indolin-2-ones compounds were synthesized and their inhibitory activities against RSK2 were evaluated. Most of these compounds showed inhibitory potential of RSK2, and the most potent one, compound **3s** showed a ~7-fold greater potency against RSK2 than the previous hit **3a**, with an IC₅₀ value of 0.5 μM. Moreover, compounds **3s** exhibited a satisfactory selectivity against 23 kinases. The structure–activity relationship (SAR) was analyzed and docking simulations were carried out to explore the binding modes of these inhibitors. Furthermore, 9 potent compounds were chosen for cellular studies. In the anti-proliferation assays on PC 3 prostate cancer cells and MCF-7 breast cancer cells, 4 compounds and 6 compounds exhibited significant inhibitions

* Corresponding authors. Tel.: +86 21 64250213 (H.L.); fax: +86 21 6425021.

E-mail addresses: zhjzhao@ecust.edu.cn (Z. Zhao), hlli@ecust.edu.cn (H. Li), yfxu@ecust.edu.cn (Y. Xu).

[†] These authors contributed equally to this work.

on proliferations of PC 3 cells and MCF-7 cells, respectively, whilst four compounds could both suppress proliferations of the two cell lines at the same digital level.

2. Results and discussion

2.1. Chemistry

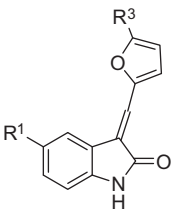
Synthesis of the compounds listed in Tables 1 and 2 is shown in Scheme 1, which involved two steps: (1) in the presence of sodium hydroxide, isatin or 5-substituted isatin was treated with hydrazine hydrate in ethanol at reflux temperature for 3–4 h to afford indolin-2-one (**2a–d**);²⁸ (2) purified indolin-2-one was dissolved in ethanol with aldehydes,^{29,30} then the mixture was heated and refluxed for 2–12 h. The precipitates were filtered to give crude products **3a–z**.²⁸ The terminal products were separated and purified by recrystallization or silica gel chromatography and the structures were characterized by ¹H NMR and HRMS (EI).

Compounds **4a–4m** in Table 3 were prepared as described in Scheme 2. The starting material was isatin or 5/7-substituted isatin with various 2-thioxothiazolidin-4-one/aromatic amines/hydrazones.³¹ The 5-(7-methyl-2-oxindolin-3-ylidene)-2-thioxothiazolidin-4-one (**4a**) and the 5-(7-ethyl-2-oxindolin-3-ylidene)-2-thioxothiazolidin-4-one (**4b**) were synthesized according to the methods presented in the literature, whereas **4c–m** were purchased from a commercial reagent company.

2.2. Structure–activity relationships

Derived from the previously discovered hit **3a**,²² structural optimizations underwent three phases, as illustrated in Figure 2. Firstly, the furan ring was reserved with the indolin-2-one scaffold, and common substituent groups were introduced onto the furan ring and the phenyl of the indolin-2-one separately or simultaneously. Secondly, the furan ring was replaced by its bioisostere pyrazole, and then similar substituent groups were studied as

Table 1
Compounds **3a–p** with RSK2 inhibitory activities

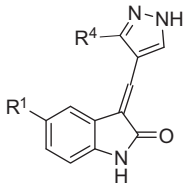


Compound	R1	R3	Inhibitory rate (%)	IC ₅₀ ^a (μM)
3a	H-	H-	69.59	3.47 ^b
3b	Cl-	H-	84.75	2.02
3c	Br-	H-	87.35	1.51
3d	H-	2-ClPh-	16.83	ND
3e	H-	3-BrPh-	21.89	ND
3f	H-	2,6-2Cl-4-CF3Ph-	<10	ND
3g	H-	O-PhthalimideCH2-	16.47	ND
3h	Br-	2-ClPh-	22.28	ND
3i	Br-	3-BrPh-	<10	ND
3j	Cl-	2-ClPh-	32.11	ND
3k	Cl-	3-BrPh-	<10	ND
3l	F-	2-ClPh-	17.12	ND
3m	F-	3-BrPh-	26.29	ND
3n	NH ₂ -	H-	100%	2.49
3o	NO ₂ -	H-	29.84%	ND
3p	CH ₃ O-	H-	25.63%	ND

^a IC₅₀ values were measured if the inhibition rate at 10 μM was larger than 50%, and ND represented not determined.

^b The IC₅₀ value of **3a** in previous report was 7.76 μM.²²

Table 2
Compounds **3q–z** with RSK2 inhibitory activities



Compound	R1	R4	Inhibitory rate (%)	IC ₅₀ ^a (μM)
3q	H-	Ph-	79.48	2.72
3r	H-	4-FPh-	38.56	ND
3s	H-	2-NO ₂ Ph	93.36	0.5
3t	F-	Ph-	78.43	8.59
3u	F-	4-FPh-	<10	ND
3v	Br-	Ph-	33.57	ND
3w	Br-	4-FPh-	<10	ND
3x	Cl-	Ph-	33.25	ND
3y	Cl-	4-FPh-	44.46	ND
3z	Cl-	4-ClPh-	<10	ND

^a IC₅₀ values were measured if the inhibition rate at 10 μM was larger than 50%, and ND represented not determined.

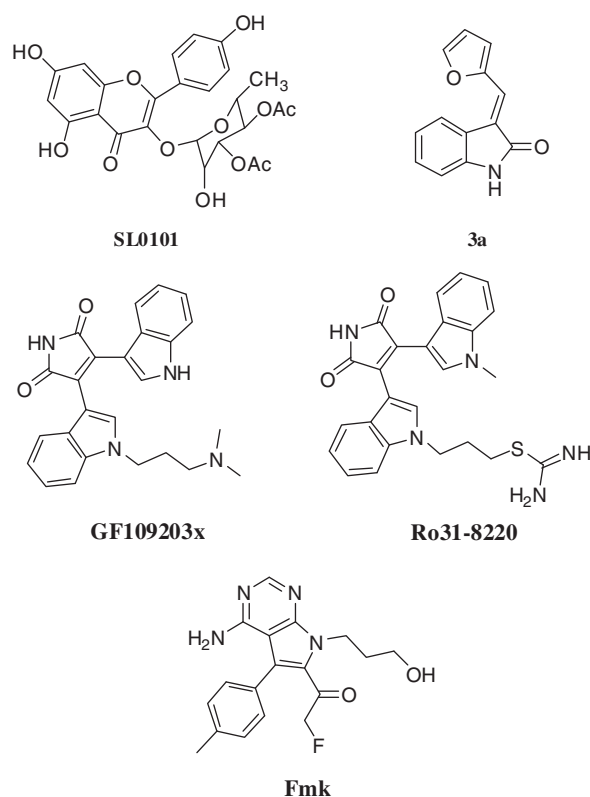
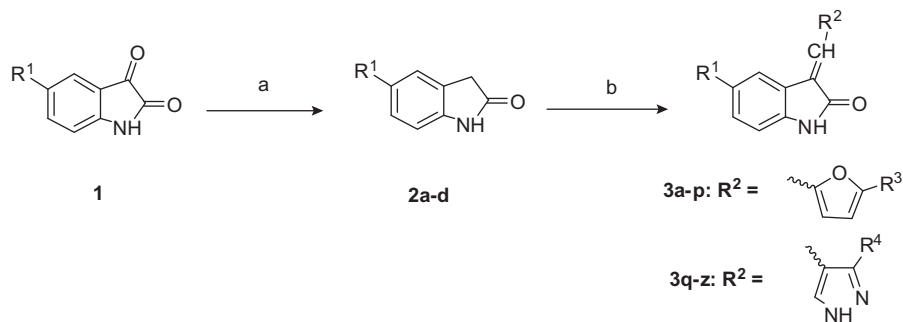


Figure 1. The reported specific RSK2 inhibitor and the hit compound **3a**.

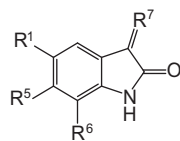
stated above. Finally, only the indolin-2-one was fixed, while various substituents were introduced onto the scaffold for diversity.

To evaluate the structure–activity relationship (SAR), the inhibitory activities against RSK2 for indolin-2-ones including synthesized ones and commercial purchased ones were analyzed and discussed (Tables 1–3). As a whole, 9 compounds (**3a–3c**, **3n**, **3q**, **3s**, **3t**, **4a**, **4b**) exhibited moderate inhibitory potencies against RSK2 with IC₅₀ values less than 10 μM, and the inhibitory potencies were substantially improved, especially compound **3s** reached a 10-fold (IC₅₀ = 0.5 μM) improvement in potency compared to the lead compound **3a**.



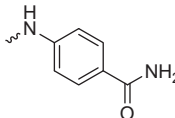
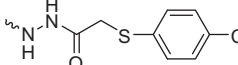
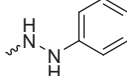
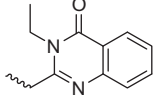
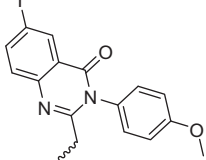
Scheme 1. Reagents and conditions: (a) Hydrazine hydrate/sodium hydroxide, EtOH/100 °C; (b) aldehydes, piperidine, EtOH/reflux.

Table 3
Compounds **4a–p** with RSK2 inhibitory activities

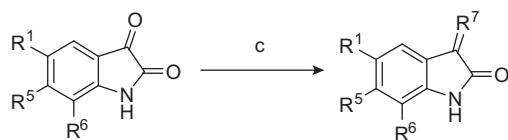


Compound	R1	R5	R6	R7	Inhibitory rate (%)	IC ₅₀ ^a (μM)
4a	H-	H-	CH ₃ -		92.36	1.68
4b	H-	H-	CH ₃ CH ₂ -		50.11	17
4c	H-	Cl-	CH ₃ -		39.58	ND
4d	H-	Cl-	H-		18.43	ND
4e	CH ₃ -	H-	H-		41.07	ND
4f	Cl-	H-	H-		<10	ND
4g	F-	H-	H-		<10	ND
4h	Br	H-	H-		11.48	ND
4i	H-	H-	H-		<10	ND
4j	Br-	H-	H-		<10	ND
4k	F-	H-	H-		30.05	ND

Table 3 (continued)

Compound	R1	R5	R6	R7	Inhibitory rate (%)	IC ₅₀ ^a (μM)
4l	H-	H-	H-		<10	ND
4m	CH ₃ CH ₂ -	H-	H-		<10	ND
4n	F-	H-	H-		<10	ND
4o	H-	H-	H-		<10	ND
4p	H-	H-	H-		13.42	ND

^a IC₅₀ values were measured if the inhibition rate at 10 μM was larger than 50%, and ND represented not determined.



Scheme 2. Reagents and conditions: (c) rhodanine/amines/hydrazone, EtOH/reflux.

In detail, modifications were first focused on common substituent groups which were introduced onto the indolin-2-one and the furan ring. Consequently comparing with **3b** and **3c** in Table 1, it was inferred that a single substituent at the 5-position of the indolin-2-one such as halogen could be accommodated which even leads to a slight improvement on the inhibitory activity. Furthermore, an amino group substituent (**3n**) could also be tolerated at the 5-position of the indolin-2-one, but the introduction of a nitro group (**3o**) or a methoxy group (**3p**) would lead to the abortion of inhibitory activities. While turning attention to the single substituent on the furan ring (**3d–3g**), we noticed that any large group at the 2-position of the furan ring would lead to an obvious decrease in the inhibitory activity against RSK2. And the deterioration in activity would be sustained when substituents were introduced onto both sites (**3h–3m**), especially, the inhibitory ratios would reduce more in the case that additional substituent groups were extended from 3-position instead of 2-position at the phenyl introduced onto the 2-position of the furan group (**3i**, **3k**). But the tendency would be reversed when it was a smaller fluorine group compared with larger chlorine or bromine groups at the 5-position of the indolin-2-one (**3m**), which was also observed in the cases of hydrogen substituents **3d** and **3e**.

Then the furan ring was replaced by a pyrazole ring and a similar investigation was undertaken. For **3q** in Table 2, we found that the replacement did not result in a big change but brought a slight boost in the activity. And the phenyl here at the 3-position of the pyrazole could be accepted, whereas additional substituents on the phenyl affected activities of derived compounds **3r** and **3s** to

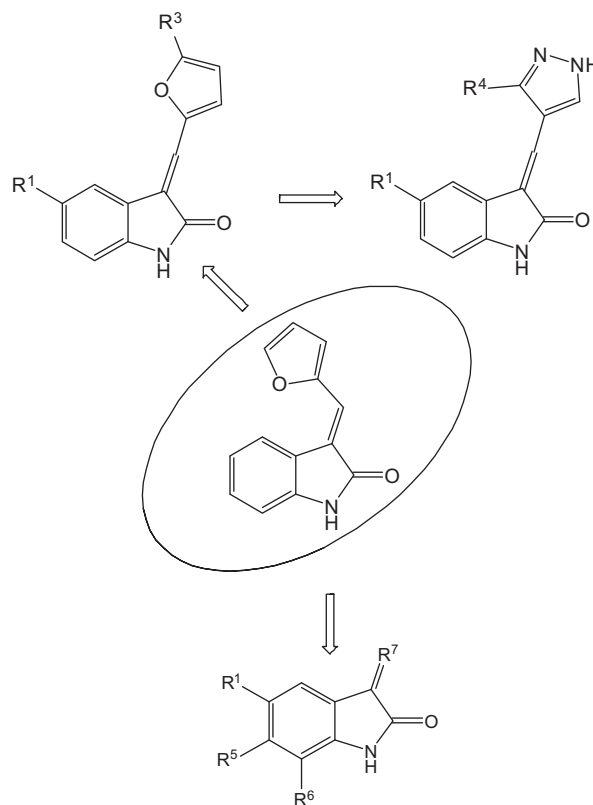


Figure 2. The structural modification progress derived from the hit **3a**.

a larger extent. The observation indicated that electron-withdrawing groups introduced onto the phenyl were accommodated, but the 2-position might be superior for the derivation. Moreover, when it was referred to **3t**, **3v** and **3x**, the introduction of an electron-withdrawing group like halogen into the 5-position

Table 4
The anti-proliferative activities of indolin-2-one compounds

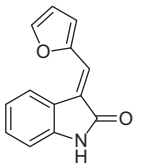
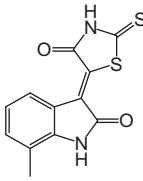
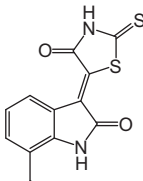
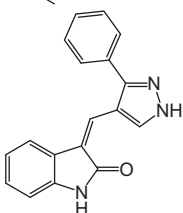
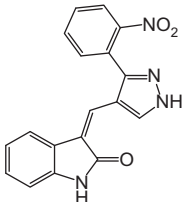
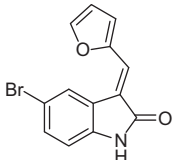
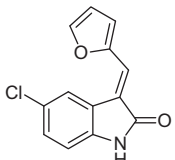
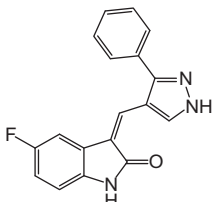
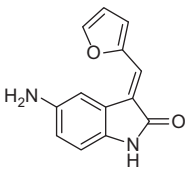
Compound	Structure	IC ₅₀ (μM) against RSK2	IC ₅₀ in PC 3 cells ^a (μM)	IC ₅₀ in MCF-7 cells ^b (μM)
3a		3.47	<10% at 100 μM	30.07
4a		1.68	<10% at 100 μM	41.46% at 100 μM
4b		17	40.89% at 100 μM	15.98% at 100 μM
3q		2.72	6.19	8.55
3s		0.5	9.32	14.84
3c		1.51	16.89	9.84
3b		2.02	23.91	14.67
3t		8.59	<10% at 100 μM	<10% at 100 μM

Table 4 (continued)

Compound	Structure	IC ₅₀ (μM) against RSK2	IC ₅₀ in PC 3 cells ^a (μM)	IC ₅₀ in MCF-7 cells ^b (μM)
3n		2.49	<10% at 100 μM	15.54
Ro31-8220			1.74	1.96

^a All measurements were determined in PC 3 prostate cancer cells. IC₅₀ values were measured if the inhibition rate at 100 μM was larger than 50%.

^b All measurements were determined in MCF-7 breast cancer cells. IC₅₀ values were measured if the inhibition rate at 100 μM was larger than 50%.

of indolin-2-one here was not beneficial to the activity but the smaller fluorine group could affect less, which was different from the observations in Table 1. As a result, with halogen groups simultaneously introduced into the 5-position of the indolin-2-one and the 4-position of the phenyl, such derivatives as **3w**, **3y** and **3z**, almost lost their inhibitory potencies against the enzyme.

Lastly, as listed in Table 3, we tried other heterocyclic and non-conjugate groups instead of the original furan group and inspected substituents at other positions on the indolin-2-one scaffold. Generally speaking, non-conjugate groups derived compounds such as **4g**, **4h**, **4m** and **4n** significantly attenuated their inhibitory activities. Since kinase inhibitors like the indolin-2-ones usually bound to the ATP site of a kinase, and mimicked the flat, hydrophobic nature of the adenine, it was supposed that the non-conjugate groups might seriously break the coplanarity of the whole molecule and thus hampered its inhibitory activity. Consequently, the 2-thioxothiazolidin-4-one derivatives showed expected superior potencies. For corresponding compounds **4a–4e**, it was clear that a substituent not larger than a methyl at the 7-position of the scaffold could be helpful, contrasting to a 10-fold decrease in the activity derived from the ethyl substituent, whereas substituents at other positions of the scaffold almost weakened activities.

2.3. Anti-proliferative activity studies

For further study, 9 potent compounds from the above enzyme assays were picked out to assess the anti-proliferation activities against the human prostate cancer cell line PC 3 and the breast cancer cell line, MCF-7. According to the data listed in Table 4 and 4 compounds and 6 compounds exhibited potent inhibitions on proliferations of PC 3 cells and MCF-7 cells, respectively, whilst 4 compounds could both suppress proliferations of the two cell lines with equivalent inhibitory activities. As to the structure, compounds of furan and pyrazole series almost showed anti-proliferation activities on at least one cancer cell line except **3t**, whereas 2-thioxothiazolidin-4-one derivatives lost inhibitory activities at the cellular level. Besides, the MCF-7 cells seemed to be more sensitive to compounds of furan series, but various substituents on the indolin-2-one scaffold didn't affect the anti-proliferation activity greatly.

2.4. Kinase profiling study

The most potent compound **3s** was further investigated for selectivity versus a panel of 23 kinases at two concentrations (Table 5). In details, at a lower concentration of 3 μM, the compound exhibited satisfactory selectivity with inhibitory rate values almost less than 50%, except for the one of 55% against c-Kit. But at a higher concentration of 10 μM, it turned to be promiscuous to multiple kinases which showed inhibitory rate values more than 50% over 12 kinases. From the inhibitory activities against kinases of different families based on the human protein kinases phylogenetic tree

Table 5

Selectivity of compound **3s** versus a panel of 23 kinases

Kinases	Inhibitory rate (%) with two compound concentrations ^a (μM)		Control IC ₅₀ ^b (nM)
	10	3	
RSK2	80%	61%	1.6
PKCα	13%	4.4%	0.98
PDK1	6.2%	6.7%	8.3
p70S6K	71%	44%	0.75
LCK	55%	31%	3.3
Lyn A	49%	25%	4.0
cKit	64%	55%	10
PIM1	4.7%	4.2%	54
FGFR3	65%	44%	25
FGFR1	65%	44%	12
PDGFRα	38%	20%	1.2
PDGFRβ	70%	41%	0.4
KDR	65%	39%	7.7
SRC	55%	30%	7.9
ABL	67%	43%	271
Aurora B	34%	25%	2.3
c-MET	16%	12%	109
MSK1	33%	31%	4.0
AKT1	8.3%	7.8%	11
JNK2	71%	36%	5028
GSK3β	40%	37%	13
p38α	27%	19%	11
ERK1	57%	31%	1146

^a Kinases selected for screening here were from Shanghai ChemPartner Co., Ltd.

^b Staurosporine and PI 103 were taken as the positive control for the kinase screening study.

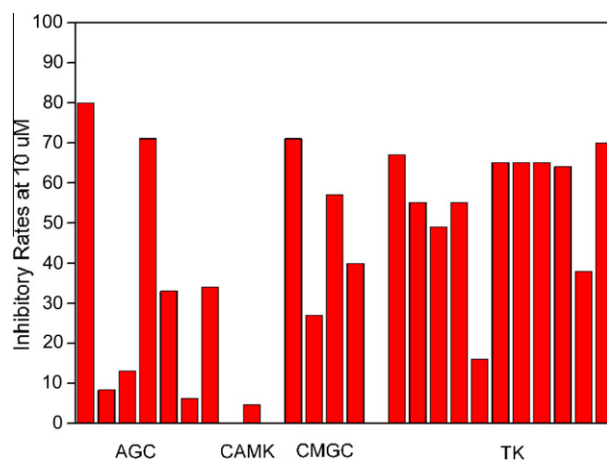


Figure 3. Selectivity of compound **3s** against 23 kinases at the concentration of 10 μM. The kinases were classified into four families based on the human protein kinases phylogenetic tree by Manning et al. And they are exhibited in orders as: RSK2, AKT1, PKCα, p70S6K, MSK1, PDK1, Aurora B, PIM1, JNK2, p38α, ERK1, GSK3β, ABL, LCK, Lyn A, SRC, c-MET, FGFR1, FGFR3, KDR, cKit, PDGFRα, PDGFRβ.

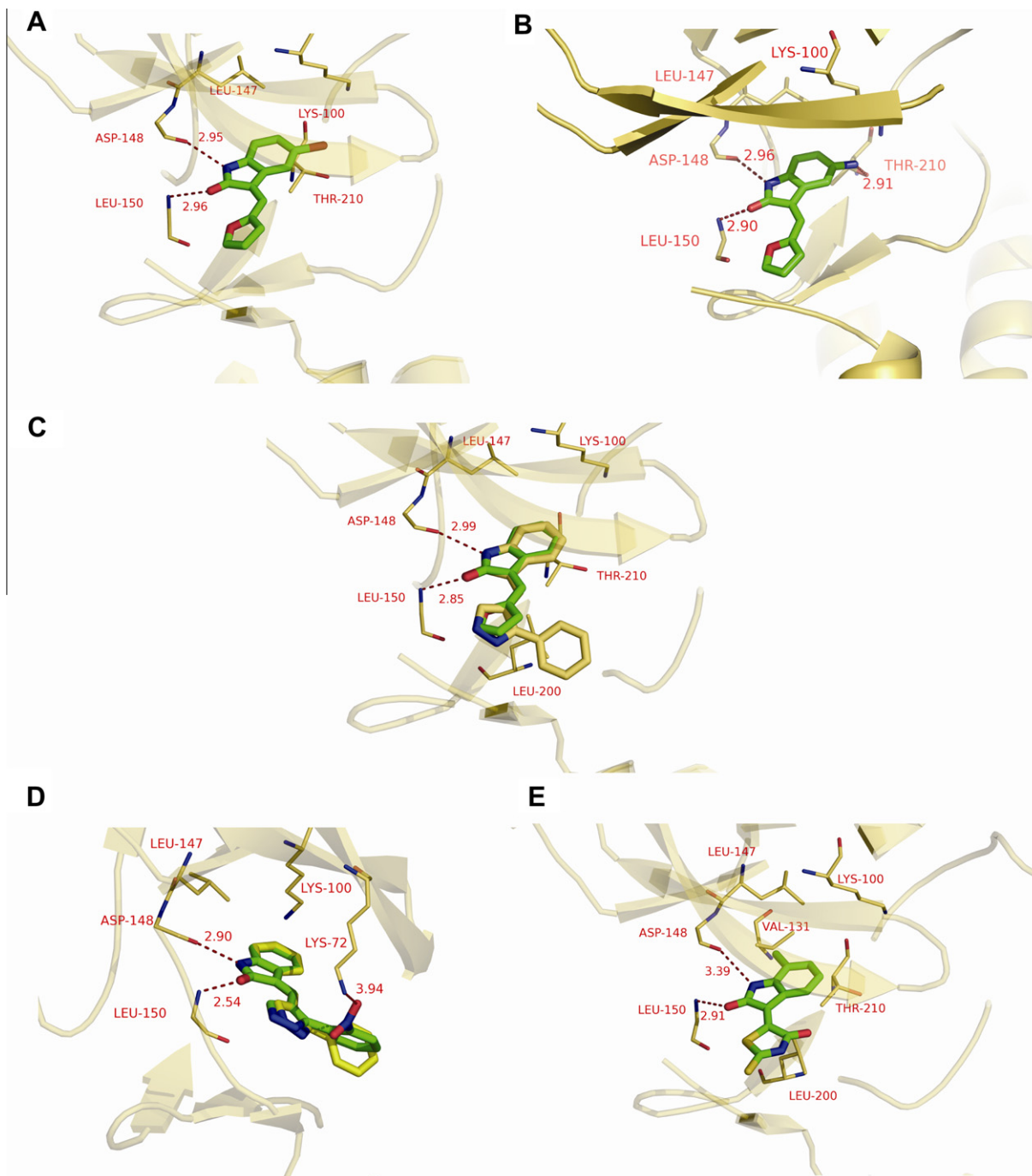


Figure 4. Binding models of the representative inhibitors. The proposed binding modes of compounds (stick, green carbon) **3c** (A), **3n** (B), **3q** (C), **3s** (D) and **4a** (E) to the RSK2 NTKD homology model (wire, yellow carbon). The nitrogen and oxygen atoms are colored in blue and red, respectively. Hydrogen atoms are hidden for clarity. Potential intermolecular hydrogen bonds are shown in red dashed lines. (C) The docked **3q** and protein residues are shown in golden, while the furan substituent lead **3a** in comparison is colored in green. (D) The docked **3s** is colored in green, whilst protein residues and **3q** are shown in yellow.

by Manning et al. (Fig. 3),³² it is found that the compound is prone to exhibit higher inhibitory activities versus members of AGC kinase family such as RSK2 and p70S6K. Interestingly, it also shows higher degree of inhibitory activities against members of TK and CMGC kinase families which are far from the AGC kinase family on the phylogenetic tree. In particular, the compound can result in an inhibitory rate value of 70% to PDGFR β , but only 38% to the homology PDGFR α . So it could be concluded that the affinity profile might not be driven by kinase homology but greatly by the chemotype of a compound, which is consistent with other reported observations.³³

2.5. Docking studies

To investigate the structural basis for the binding of the indolin-2-ones to the RSK2 NTKD ATP-binding site, the compounds **3c**, **3n**, **3q**, **3s** and **4a** were picked out for the docking simulation and the binding poses of them were proposed, as illustrated in Figure 4. Although there have been two crystal structures of RSK2 NTKD complexed with inhibitors which have been released recently, the ligands in the complexes are almost identical to each other but very different from the indolin-2-one series here, which are reported to induce the protein moiety to make unprecedented

structural rearrangements.¹⁹ In addition, in many other reports on the indolin-2-one scaffold as kinase inhibitors, it was found that the scaffold bound to kinases nearly in the same way as the interactions of staurosporine to kinases.^{27,34–41} Thus we herein used the previously reported RSK2 NTKD homology model complexed with staurosporine.

In consistent with other RSK2 inhibitors we reported previously,²² **3c** binds to the enzyme in a similar manner (Fig. 4A), except that the bromine at 5-position of the indolin-2-one extends into a hydrophobic pocket constituted by Leu 147, Lys 100 and Thr 210. In the case of **3n** (Fig. 4B), it keeps the key hydrogen bond interactions like **3c** and formed an additional hydrogen bond with Thr 210 as a donor. Thus the inhibitory activities of the nitro group and the methoxy group substituent derivatives (**3o** and **3p**) were attenuated greatly. In addition, by the superimposition of **3a** and **3q** in Figure 4C, it should be noted that the furan ring located close to the entrance of the ATP binding pocket, thus a large substituent like a phenyl at the other α position of the furan ring may make the molecule stretch beyond the pocket. Thus such derivatives as **3d–3m** lost activities dramatically.

As for the pyrazole replaced **3q** (Fig. 4C), the indolin-2-one scaffold is found to form two hydrogen bonds with the hinge residues Asp 148 and Leu 150 as it is in the lead **3a**, and the pyrazole occupies the same location but with different angles as the furan; moreover, the extended phenyl here can contact the protein by VDW interactions with Leu 200 which therefore is helpful to the activity. Besides, noting that pyrazole derivatives (**3q**) exhibit superior planarity to furan ones (**3a**) in Figure 4C, which probably reflects the electronic conjugate profile in the former is more complete. Thus substituent electron-withdrawing groups like halogen atoms in pyrazole ones would reduce the electronic distribution in the whole conjugate system efficiently to attenuate the key hydrogen bond to Leu 150 and further result in a decrease in activities. Accordingly, halogen substituents in the 5-position of indolin-2-one here could impair binding affinities by intense electron-withdrawing effects, especially Cl- and Br- ones (**3x** and **3v**), compared to those in furan series, might exhibit less electron-withdrawing effects but more hydrophobic effects (**3b** and **3c**). With respect to the analogue **3s** (Fig. 4D), it conserves the basic interaction profile of **3q**, but the nitro group at the 2-position of the phenyl can destroy planarity of the whole molecule and form an additional hydrogen bond with Lys 72, thus force the molecule to shift close to the hinge with the corresponding hydrogen bond distances shorten from 2.99 Å and 2.85 Å induced by **3q** to 2.90 Å and 2.54 Å here (Fig. 4C), which may both make significant contributions to the great improvement in the activity for **3s**.

Similar to the above analysis, **4a** binds to the enzyme in the same region of the ATP binding site (Fig. 4E), noting that the methyl at the 7-position of the indolin-2-one scaffold fits well into the binding site to form VDW interactions and hydrophobic effects with the residues Leu 147 and Val 131. Meanwhile, the hydrophobic sub-pocket comprised by the referred residues is found to be small and hard to accommodate groups larger than a methyl, so the ethyl substituent results in an intense decrease in the activity of **4b**.

3. Conclusions

In summary, through structural optimizations of the previously identified hit, a series of indolin-2-ones analogues were designed and synthesized as potential RSK2 inhibitors. Most of these compounds showed potential RSK2 inhibitory activity, and the most potent one, compound **3s** showed a \sim 7-fold increased activity than hit compound, with the IC₅₀ value of 0.5 μ M. In addition, the compound **3s** exhibited a satisfactory selectivity versus 23 kinases

at a lower concentration of 3 μ M, but it showed inhibitory rate values more than 50% over 12 compounds at a higher concentration of 10 μ M. The proposed binding modes of these compounds were subsequently explored to elucidate their SAR. Furthermore, cellular assays confirmed that 4 compounds and 6 compounds exhibited significant inhibitions on proliferations of PC 3 cells and MCF-7 cells, respectively, whilst 4 compounds could both suppress proliferations of the two cell lines in the same digital level. To the best of our knowledge, there are no public reports that indoline-2-ones can act as RSK2 inhibitors, which exhibited moderate or potent potencies. Therefore, the challenge remains to identify derivatives which show greater potency and serve as novel lead compounds for further development of therapeutics to treat cancer, especially to suppress cell migration.

4. Experimental section

4.1. Chemistry

4.1.1. General methods

All reagents were commercial quality without further purification. Solvents were analytical grade, and were subsequently purified and dried by standard methods according to reaction conditions. ¹H NMR and ¹³C NMR were measured on a Bruker AV-400 spectrometer using TMS as internal standard. The chemical shifts were reported as ppm (in DMSO-*d*₆, CD₃OD). Melting points were measured on an X6 apparatus, which were uncorrected. High-resolution EI mass spectra were reported on a HPLC-Q-ToF MS (Micro) spectrometer. All the compounds were visualized by UV illumination (254 nm). Analytical thin-layer chromatography was performed with glass-baked silica gel plates. HPLC was performed by using a Zorbax RX-C18 column (packing: 5 μ m, 4.6 \times 150 mm) with a mobile phase consisting of H₂O/CH₃CN at a flow rate of 1.0 mL/min. All stereochemistry were confirmed according to synthesis methods reported by Sun et al.²⁸

4.1.2. Method A: General procedure for the preparation of compounds **3a–o**

The preparation was divided into two steps. Firstly, substituent indoline-2,3-dione (1 equiv) was dissolved in ethanol (10 mL), hydrazine hydrate (2 mL) was added. The reaction mixture was refluxed with magnetic stirring for 3 h and cooled to 0 °C, then sodium hydroxide (3 equiv) was added, refluxed for 0.5 h and cooled to room temperature, then 150 mL water was added. The mixture was acidified by adding 2 N hydrochloric acid to pH 2, and extracted twice with dichloromethane. The organic filtrate was washed twice with brine, dried (Na₂SO₄), and then concentrated to give corresponding indolin-2-one by high-vacuum drying. Secondly, a mixture of the corresponding indolin-2-one (1 equiv) and furan-2-carbaldehyde (1 equiv) in ethanol was added two drops of piperidine and refluxed with magnetic stirring for 5 h. After the mixture cooled, the precipitate was filtered, washed with cold ethanol, dried, and recrystallized from methanol to afford the terminal product.

4.1.2.1. (E)-6-Chloro-3-(furan-2-ylmethylene)indolin-2-one (**3b**)

Yellow powder (yield 45%), mp: 253–254 °C, ¹H NMR (400 MHz, DMSO-*d*₆) δ 10.87 (s, 1H), 8.31 (d, *J* = 2.0 Hz, 1H), 8.27 (d, *J* = 1.2 Hz, 1H), 7.41 (s, 1H), 7.34 (d, *J* = 3.2 Hz, 1H), 7.32–7.30 (m, 1H), 6.89 (d, *J* = 8.0 Hz, 1H), 6.84 (dd, *J*₁ = 1.6 Hz, *J*₂ = 3.6 Hz, 1H); ¹³C NMR (100 MHz, DMSO-*d*₆) δ 169.47, 150.96, 148.47, 141.74, 129.55, 125.81, 124.28, 123.35, 122.61, 121.44, 121.20, 114.25, 111.51; HRMS (EI) [M]⁺: Calcd for C₁₃H₈NO₂Cl: 245.0244, Found: 245.0244.

4.1.2.2. (E)-6-Bromo-3-(furan-2-ylmethylene) indolin-2-one (3c). Yellow powder (yield 72%), mp: 260–261 °C, ¹H NMR (400 MHz, DMSO-*d*₆) δ 10.71 (s, 1H), 8.44 (d, *J* = 1.6 Hz, 1H), 8.27 (s, 1H), 7.45–7.42 (m, 1H), 8.27 (s, 1H), 7.34 (d, *J* = 3.6 Hz, 1H), 6.87–6.84 (m, 2H). HRMS (EI) [M]⁺: Calcd for C₁₃H₈NO₂Br: 288.9738, Found: 288.9733.

4.1.2.3. 3-((5-(2-Chlorophenyl)furan-2-yl)methylene)indolin-2-one (3d). Orange powder (yield 90%), mp: 250–251 °C, ¹H NMR (400 MHz, DMSO-*d*₆) δ 10.60 (s, 1H), 8.39 (d, *J* = 7.6 Hz, 1H), 8.02–7.99 (m, 1H), 7.68 (d, *J* = 8.0 Hz, 1H), 7.61–7.57 (m, 1H), 7.52–7.48 (m, 1H), 7.45 (d, *J* = 3.6 Hz, 1H), 7.38–7.36 (m, 2H), 7.27 (t, *J* = 7.6 Hz, 1H), 7.01 (t, *J* = 7.6 Hz, 1H), 6.90 (d, *J* = 7.6 Hz, 1H); ¹³C NMR (100 MHz, DMSO-*d*₆) δ 169.58, 153.69, 151.22, 142.93, 131.60, 130.98, 130.61, 130.42, 128.72, 128.45, 128.24, 124.48, 123.28, 123.12, 121.72, 119.20, 115.14, 110.31; HRMS (EI) [M]⁺: Calcd for C₁₉H₁₂NO₂Cl: 321.0557, Found: 321.0560.

4.1.2.4. 3-((5-(3-Bromophenyl)furan-2-yl)methylene)indolin-2-one (3e). Citrus red powder (yield 90%), mp: 256–257 °C, ¹H NMR (400 MHz, CD₃OD) δ 10.60 (s, 1H), 8.44 (d, *J* = 8.0 Hz, 1H), 8.12 (s, 1H), 7.91 (d, 1H), 7.63 (d, *J* = 8.4 Hz, 1H), 7.54–7.51 (m, 1H), 7.45 (d, *J* = 3.6 Hz, 1H), 7.41 (d, *J* = 3.6 Hz, 1H), 7.34 (s, 1H), 7.31 (t, *J* = 7.6 Hz, 1H), 7.09 (t, *J* = 7.6 Hz, 1H), 6.92 (d, *J* = 8.0 Hz, 1H); ¹³C NMR (100 MHz, DMSO-*d*₆) δ 169.60, 155.61, 151.52, 142.90, 132.01, 131.75, 130.42, 126.95, 123.96, 123.83, 123.32, 123.09, 122.82, 121.76, 121.51, 119.17, 111.82, 110.41; HRMS (EI) [M]⁺: Calcd for C₁₉H₁₂NO₂Br: 365.0051, Found: 365.0055.

4.1.2.5. (Z)-5-Bromo-3-((5-(2-chlorophenyl)furan-2-yl)methylene) indolin-2-one (3h). Citrus red powder (yield 92%), mp: 279–280 °C, ¹H NMR (400 MHz, DMSO-*d*₆) δ 10.74 (s, 1H), 8.61 (d, *J* = 1.6 Hz, 1H), 8.07 (dd, *J*₁ = 1.2 Hz, *J*₂ = 8.0 Hz, 1H), 7.68 (d, *J* = 8.0 Hz, 1H), 7.60–7.56 (m, 1H), 7.52–7.50 (m, 2H), 7.45–7.43 (m, 3H), 6.86 (d, *J* = 8.4 Hz, 1H); ¹³C NMR (100 MHz, DMSO-*d*₆) δ 169.21, 154.16, 150.95, 141.88, 132.42, 131.63, 131.13, 130.65, 128.59, 128.43, 127.88, 126.71, 124.66, 123.77, 121.72, 120.44, 115.36, 113.53, 112.036; HRMS (EI) [M]⁺: Calcd for C₁₉H₁₁NO₂ClBr: 400.9641, Found: 400.9643.

4.1.2.6. 5-Bromo-3-((5-(3-bromophenyl)furan-2-yl)methylene) indolin-2-one (3i). Citrus red powder (yield 89%), mp: 275–276 °C, ¹H NMR (400 MHz, DMSO-*d*₆) δ 10.74 (s, 1H), 8.63 (d, *J* = 1.6 Hz, 1H), 8.14 (s, 1H), 7.98 (d, *J* = 7.6 Hz, 1H), 7.65 (d, *J* = 8.4 Hz, 1H), 7.54–7.46 (m, 4H), 7.40 (s, 1H), 6.88 (d, *J* = 8.4 Hz, 1H); ¹³C NMR (100 MHz, DMSO-*d*₆) δ 169.22, 156.40, 151.39, 141.79, 132.53, 132.35, 131.82, 131.51, 126.89, 126.26, 125.36, 123.87, 123.55, 123.35, 121.28, 120.43, 113.46, 112.16, 112.12; HRMS (EI) [M]⁺: Calcd for C₁₉H₁₁NO₂Br₂: 444.9136, Found: 444.9144.

4.1.2.7. (Z)-5-Chloro-3-((5-(2-chlorophenyl)furan-2-yl)methylene)indolin-2-one (3j). Citrus red powder (yield 86%), mp: 286–287 °C, ¹H NMR (400 MHz, DMSO-*d*₆) δ 10.73 (s, 1H), 8.49 (d, *J* = 2.0 Hz, 1H), 8.07 (dd, *J*₁ = 1.6 Hz, *J*₂ = 7.6 Hz, 1H), 7.69 (dd, *J*₁ = 1.2 Hz, *J*₂ = 7.6 Hz, 1H), 7.56–7.49 (m, 3H), 7.44 (s, 1H), 7.42 (d, *J* = 3.6 Hz, 1H), 7.32 (dd, *J*₁ = 2.0 Hz, *J*₂ = 8.4 Hz, 1H), 6.91 (d, *J* = 8.0 Hz, 1H); ¹³C NMR (100 MHz, DMSO-*d*₆) δ 169.35, 154.20, 151.00, 141.53, 131.63, 131.22, 130.74, 129.65, 128.71, 128.30, 128.00, 125.85, 124.57, 124.11, 121.91, 120.50, 115.33, 111.52; HRMS (EI) [M]⁺: Calcd for C₁₉H₁₁NO₂Cl₂: 355.0167, Found: 355.0168.

4.1.2.8. 3-((5-(3-Bromophenyl)furan-2-yl)methylene)-5-chloro-indolin-2-one (3k). Citrus red powder (yield 90%), mp: 289–290 °C, ¹H NMR (400 MHz, DMSO-*d*₆) δ 10.72 (s, 1H), 8.47 (d,

J = 2.0 Hz, 1H), 8.11 (s, 1H), 7.95 (d, *J* = 8.0 Hz, 1H), 7.64 (d, *J* = 8.8 Hz, 1H), 7.51–7.47 (m, 3H), 7.39 (s, 1H), 7.33 (dd, *J*₁ = 2.0 Hz, *J*₂ = 8.0 Hz, 1H), 6.91 (d, *J* = 8.0 Hz, 1H); HRMS (EI) [M]⁺: Calcd for C₁₉H₁₁NO₂ClBr: 400.9641, Found: 400.9639.

4.1.2.9. (E)-5-Amino-3-(furan-2-ylmethylene) indolin-2-one (3n). The reduction product of **3o**. Red powder (yield 80%), mp: 177.8–178.0 °C, ¹H NMR (400 MHz, DMSO-*d*₆) δ 10.08 (s, 1H), 8.02 (s, 1H), 7.75 (d, *J* = 1.2 Hz, 1H), 7.23 (s, 1H), 7.20–7.19 (d, *J* = 3.6 Hz, 2H), 6.80–6.79 (m, 1H), 6.57–6.51 (m, 2H); ¹³C NMR (100 MHz, DMSO-*d*₆) δ 169.60, 151.27, 146.94, 143.75, 133.75, 124.10, 122.25, 120.19, 118.89, 115.83, 113.85, 112.09, 110.27; HRMS (EI) [M]⁺: Calcd for C₁₃H₁₀N₂O₂: 226.0742, Found: 226.0743.

4.1.2.10. (E)-3-(Furan-2-ylmethylene)-5-nitroindolin-2-one (3o). Yellow powder (56%), mp: 305.8–306.3 °C, ¹H NMR (400 MHz, DMSO-*d*₆) δ 11.26 (s, 1H), 9.10 (d, *J* = 2.0 Hz, 1H), 8.25 (s, 1H), 8.16 (dd, *J*₁ = 2.4 Hz, *J*₂ = 8.4 Hz, 1H), 7.45 (s, 1H), 7.39 (d, *J* = 3.2 Hz, 1H), 7.00 (d, *J* = 8.8 Hz, 1H), 6.87–6.85 (m, 1H); ¹³C NMR (100 MHz, DMSO-*d*₆) δ 169.96, 150.84, 148.80, 148.43, 142.34, 126.31, 123.63, 122.24, 121.972, 120.26, 119.81, 114.57, 110.05; HRMS (EI) [M]⁺: Calcd for C₁₃H₈N₂O₄: 256.0484, Found: 256.0486.

4.1.2.11. (E)-3-(Furan-2-ylmethylene)-5-methoxyindolin-2-one (3p). Brown powder (yield 60%), mp: 201.8–202.8 °C, ¹H NMR (400 MHz, DMSO-*d*₆) δ 10.37 (s, 1H), 8.22 (s, 1H), 8.00 (d, *J* = 2.0 Hz, 1H), 7.34 (s, 1H), 7.27 (d, *J* = 3.2 Hz, 1H), 6.87 (dd, *J*₁ = 2.4 Hz, *J*₂ = 8.4 Hz, 1H), 6.82–6.78 (m, 2H), 3.79 (s, 3H); ¹³C NMR (100 MHz, DMSO-*d*₆) δ 169.77, 154.92, 151.14, 147.86, 136.81, 123.11, 122.54, 121.44, 119.92, 115.21, 114.01, 111.45, 110.39; HRMS (EI) [M]⁺: Calcd for C₁₄H₁₁NO₃: 241.0739, Found: 241.0736.

4.1.2.12. (Z)-3-((3-Phenyl-1H-pyrazol-4-yl)methylene) indolin-2-one (3q). Light yellow powder (yield 87%), mp: 228–229 °C, ¹H NMR (400 MHz, DMSO-*d*₆) δ 13.65 (br, 1H), 10.53 (s, 1H), 8.37 (br, 1H), 7.79 (d, *J* = 7.6 Hz, 1H), 7.59 (d, *J* = 6.8 Hz, 2H), 7.56–7.52 (m, 2H), 7.49–7.47 (m, 1H), 7.40 (s, 1H), 7.25–7.21 (m, 1H), 6.97–6.94 (m, 1H), 6.88 (d, *J* = 7.6 Hz, 1H); HRMS (EI) [M]⁺: Calcd for C₁₈H₁₃N₃O: 287.1059, Found: 287.1062.

4.1.2.13. (Z)-3-((3-(2-Nitrophenyl)-1H-pyrazol-4-yl)methylene) indolin-2-one (3s). Light yellow powder (yield 90%), mp: 263–264 °C, ¹H NMR (400 MHz, DMSO-*d*₆) δ 13.58 (br, 1H), 10.62 (s, 1H), 9.41 (s, 1H), 8.10–8.08 (m, 1H), 7.89–7.86 (m, 1H), 7.81–7.75 (m, 1H), 7.70 (dd, *J*₁ = 1.2 Hz, *J*₂ = 7.6 Hz, 1H), 7.34 (d, *J* = 7.2 Hz, 1H), 7.21–7.15 (m, 2H), 6.91 (t, *J* = 7.6 Hz, 1H), 6.84 (d, *J* = 7.6 Hz, 1H); HRMS (EI) [M]⁺: Calcd for C₁₈H₁₂N₄O₃: 332.0909, Found: 332.0909.

4.1.2.14. (Z)-5-Fluoro-3-((3-phenyl-1H-pyrazol-4-yl)methylene) indolin-2-one (3t). Orange powder (yield 92%), mp: 259–260 °C, ¹H NMR (400 MHz, DMSO-*d*₆) δ 13.79 (br, 1H), 10.80 (s, 1H), 8.76 (s, 1H), 8.52 (br, 1H), 7.01–7.69 (m, 3H), 7.54–7.52 (m, 3H), 7.25–7.20 (m, 1H), 6.87 (dd, *J*₁ = 4.0 Hz, *J*₂ = 4.4 Hz, 1H); ¹³C NMR (100 MHz, DMSO-*d*₆) δ 165.42, 159.15, 156.79, 150.87, 150.85, 141.43, 129.34, 129.07, 120.21, 119.98, 117.62, 117.53, 116.12, 115.87, 114.10, 111.98, 111.91; HRMS (EI) [M]⁺: Calcd for C₁₈H₁₂N₃OF: 305.0964, Found: 305.0969.

4.1.3. Method B: General procedure for the preparation of compounds 4a–o

Substituent indoline-2,3-dione (1 equiv) and 2-thioxothiazolidin-4-one (1 equiv) were dissolved in 5 mL ethanol, then refluxed for 10 h. After cooling to the room temperature, the precipitate

was filtered, washed with ethanol, dried, and recrystallized from methanol to afford the terminal product.

4.1.3.1. (Z)-5-(7-Methyl-2-oxoindolin-3-ylidene)-2-thioxothiazolidin-4-one (4a). Black powder (yield 53%), mp >300 °C, ¹H NMR (400 MHz, CD₃OD) δ 8.77 (d, *J* = 8.0 Hz, 1H), 7.23 (d, *J* = 8.0 Hz, 1H), 7.01–6.97 (m, 1H), 2.29 (s, 3H); HRMS (EI) [M]⁺: Calcd for C₁₂H₈N₂O₂S₂: 276.0027, Found: 276.0029.

4.1.3.2. (Z)-5-(7-Ethyl-2-oxoindolin-3-ylidene)-2-thioxothiazolidin-4-one (4b). Black powder (yield 65%), mp >300 °C, ¹H NMR (400 MHz, CD₃OD) δ 8.80 (dd, *J*₁ = 0.4 Hz, *J*₂ = 7.6 Hz, 1H), 7.27 (d, *J* = 7.2 Hz, 1H), 7.05–7.01 (m, 1H), 2.65 (q, *J* = 7.6 Hz, 2H) 1.24 (t, *J* = 7.6 Hz, 3H); HRMS (EI) [M]⁺: Calcd for C₁₃H₁₀N₂O₂S₂: 290.0184, Found: 290.0185.

4.2. In vitro kinase inhibition assay

The kinase inhibition assay was performed as described previously.²² The ADP Quest[®] kinase assay kits were purchased from DiscoverX. The Kinase in 40 μL assay buffer (15 mM HEPES, pH 7.4, 20 mM NaCl, 1 mM EGTA, 0.02% Tween 20, 10 mM MgCl₂, and 0.1 mg/mL BGG (bovine-γ-globulins) containing 25 μM S6 peptide substrate (AKRRRLSSLR) was incubated for 20 min at room temperature with varied concentrations of the compounds to be tested. Reactions were started by the addition of 10 μL of ATP (a final concentration of 10 μM). Reactions were stopped after 60 min by the addition of 20 μL ADP Reagent A and 40 μL ADP Reagent B, respectively. Ro31-8220 was used as the positive control. Compounds were prepared from stock in DMSO and diluted to different concentration with assay buffer. The fluorescence signal, which detected the amount of ADP produced as a result of enzyme activity was recorded on the Synergy[™]2 Multi-Mode Microplate Reader (BioTek) at an excitation wavelength of 530 nm and an emission wavelength of 590 nm at 30 min after the addition of the ADP Reagent B. IC₅₀ values were determined by using the GraphPad Prism software with three independent determinations.

4.3. MTT assays

The anti-proliferative activity of RSK2 inhibitors picked out was measured by the MTT assay as previously described with some modification.²² Human breast cancer MCF-7 cells (5 × 10³) were cultured in 96-well plates with 200 μL of DMEM plus 10% FBS medium (Invitrogen) and incubated with compounds at various concentrations. And human prostate cancer PC 3 cells (5 × 10³) were seeded in 96-well plates with 200 μL of F-12K medium (Invitrogen) to be treated in the same way. Ro31-8220 was used as a positive comparison. After 48 h incubation, the cells were added with 10 μL of 5 mg/mL 3-[4,5-dimethylthiazol-2-yl]-2,5-diphenyl tetrazolium bromide (MTT) at 37 °C in a humidified incubator with 5% CO₂ for another 4 h. Then the formazan crystals were dissolved in 150 μL DMSO, and the absorbance was measured at 570 nm by using a Synergy 2 multimode microplate reader (BioTek, USA). IC₅₀ values were obtained from the results of three independent experiments and calculated from the inhibition curves.

4.4. Kinase profiling study with compound 3s

The details for the testing process are given in the Supplementary data.

4.5. Molecular docking

The 3D structures of the compounds were prepared by the Ligprep module in Maestro (Schrödinger Inc., version 7.5) with

the default parameters, while the RSK2 NTKD homology model was previously reported by our group elsewhere.²² Then GLIDE program was chosen to perform the molecular docking simulation. With the default parameter sets, the grid-enclosing box was centered on the centroid of the ligand in the RSK2 homology model and defined so as to enclose residues within 20 Å around the ATP binding site, and a scaling factor of 1.0 was set to van der Waals (VDW) radii of those receptor atoms with the partial atomic charge less than 0.25. The Extra-precision (XP) mode of GLIDE was taken to ensure the docking, and the top 10 docked poses of each compound were reserved for further analysis.

Acknowledgments

This work was supported by the Fundamental Research Funds for the Central Universities, the National Natural Science Foundation of China (Grants 21173076, 81102375, 10979072, 81230090, 81222046 and 81230076), the Special Fund for Major State Basic Research Project (Grant 2009CB918501), the Shanghai Committee of Science and Technology (Grants 09dZ1975700, 11DZ2260600 and 10431902600), the 863 Hi-Tech Program of China (Grant 2012AA020308) and the National S&T Major Project of China (Grant 2011ZX09307-002-03). Honglin Li is also sponsored by Program for New Century Excellent Talents in University (Grant NCET-10-0378).

Supplementary data

Supplementary data (the details of the testing process for kinase profile study on 3s) associated with this article can be found, in the online version, at <http://dx.doi.org/10.1016/j.bmc.2013.01.047>.

References and notes

- Jones, S. W.; Erikson, E.; Blenis, J.; Maller, J. L.; Erikson, R. *Proc. Natl. Acad. Sci. U.S.A.* **1988**, *85*, 3377.
- Anjum, R.; Blenis, J. *Nat. Rev. Mol. Cell Biol.* **2008**, *9*, 747.
- Carriere, A.; Ray, H.; Blenis, J.; Roux, P. P. *Front. Biosci.* **2008**, *13*, 4258.
- Cho, Y. Y.; Yao, K.; Bode, A. M.; Bergen, H. R.; Madden, B. J.; Oh, S. M.; Ermakova, S.; Kang, B. S.; Choi, H. S.; Shim, J. H. *J. Biol. Chem.* **2007**, *282*, 8380.
- Xing, J.; Ginty, D. D.; Greenberg, M. E. *Science* **1996**, *273*, 959.
- Yang, X.; Matsuda, K.; Bialek, P.; Jacquot, S.; Masuoka, H. C.; Schinke, T.; Li, L.; Brancorsini, S.; Sassone-Corsi, P.; Townes, T. M. *Cell* **2004**, *117*, 387.
- Cho, Y. Y.; Yao, K.; Kim, H. G.; Kang, B. S.; Zheng, D.; Bode, A. M.; Dong, Z. *Cancer Res.* **2007**, *67*, 8104.
- Doehn, U.; Hauge, C.; Frank, S. R.; Jensen, C. J.; Duda, K.; Nielsen, J. V.; Cohen, M. S.; Johansen, J. V.; Winther, B. R.; Lund, L. R. *Mol. Cell* **2009**, *35*, 511.
- Peng, C.; Cho, Y. Y.; Zhu, F.; Xu, Y. M.; Wen, W.; Ma, W. Y.; Bode, A. M.; Dong, Z. *FASEB J.* **2010**, *24*, 3490.
- Kang, S.; Chen, J. *Expert Opin. Ther. Targets* **2011**, *15*, 11.
- Smith, J. A.; Maloney, D. J.; Clark, D. E.; Xu, Y.; Hecht, S. M.; Lannigan, D. A. *Bioorg. Med. Chem.* **2006**, *14*, 6034.
- Smith, J. A.; Maloney, D. J.; Hecht, S. M.; Lannigan, D. A. *Bioorg. Med. Chem.* **2007**, *15*, 5018.
- Smith, J. A.; Poteet-Smith, C. E.; Xu, Y.; Errington, T. M.; Hecht, S. M.; Lannigan, D. A. *Cancer Res.* **2005**, *65*, 1027.
- Alessi, D. R. *FEBS Lett.* **1997**, *402*, 121.
- Nguyen, T. L. *Anti-Cancer Agents Med. Chem.* **2008**, *8*, 710.
- Sapkota, G. P.; Cummings, L.; Newell, F. S.; Armstrong, C.; Bain, J.; Frodin, M.; Grauert, M.; Hoffmann, M.; Schnapp, G.; Steegmaier, M. *Biochem. J.* **2007**, *401*, 29.
- Cohen, M. S.; Zhang, C.; Shokat, K. M.; Taunton, J. *Science* **2005**, *308*, 1318.
- Cohen, M. S.; Hadjivassiliou, H.; Taunton, J. *Nat. Chem. Biol.* **2007**, *3*, 156.
- Utepergenov, D.; Derewenda, U.; Olekhovich, N.; Szukalska, G.; Banerjee, B.; Hilinski, M. K.; Lannigan, D. A.; Stukenberg, P. T.; Derewenda, Z. S. *Biochemistry* **2012**, *51*, 6499.
- Lu, W.; Liu, X.; Cao, X.; Xue, M.; Liu, K.; Zhao, Z.; Shen, X.; Jiang, H.; Xu, Y.; Huang, J.; Li, H. *J. Med. Chem.* **2011**, *54*, 3564.
- Liu, X.; Jiang, H.; Li, H. *J. Chem. Inf. Model.* **2011**, *51*, 2372.
- Li, S.; Zhou, Y.; Lu, W.; Zhong, Y.; Song, W.; Liu, K.; Huang, J.; Zhao, Z.; Xu, Y.; Liu, X.; Li, H. *J. Chem. Inf. Model.* **2011**, *51*, 2939.
- Xue, M.; Xu, M.; Lu, W.; Huang, J.; Li, H.; Xu, Y.; Liu, X.; Zhao, Z. *J. Enzyme Inhib. Med. Chem.* **2012**. <http://dx.doi.org/10.3109/14756366.2012.681651>.
- Rellos, P.; Ivins, F. J.; Baxter, J. E.; Pike, A.; Nott, T. J.; Parkinson, D. M.; Das, S.; Howell, S.; Fedorov, O.; Shen, Q. Y. *J. Biol. Chem.* **2007**, *282*, 6833.

25. Gajiwala, K. S.; Wu, J. C.; Christensen, J.; Deshmukh, G. D.; Diehl, W.; DiNitto, J. P.; English, J. M.; Greig, M. J.; He, Y. A.; Jacques, S. L. *Proc. Natl. Acad. Sci. U.S.A.* **2009**, *106*, 1542.
26. Zhu, G. D.; Gandhi, V. B.; Gong, J.; Luo, Y.; Liu, X.; Shi, Y.; Guan, R.; Magnone, S. R.; Klinghofer, V.; Johnson, E. F. *Bioorg. Med. Chem. Lett.* **2006**, *16*, 3424.
27. Moshinsky, D. J.; Bellamacina, C. R.; Boisvert, D. C.; Huang, P.; Hui, T.; Jancarik, J.; Kim, S. H.; Rice, A. G. *Biochem. Biophys. Res. Commun.* **2003**, *310*, 1026.
28. Sun, L.; Tran, N.; Tang, F.; App, H.; Hirth, P.; McMahon, G.; Tang, C. J. *Med. Chem.* **1998**, *41*, 2588.
29. Katritzky, A. R.; Tala, S. R.; Lu, H.; Vakulenko, A. V.; Chen, Q. Y.; Sivapackiam, J.; Pandya, K.; Jiang, S.; Debnath, A. K. *J. Med. Chem.* **2009**, *52*, 7631.
30. Lebedev, A.; Lebedeva, A.; Sheludyakov, V.; Kovaleva, E.; Ustinova, O.; Kozhevnikov, I. *Russ. J. Gen. Chem.* **2005**, *75*, 782.
31. Sridhar, S. K.; Saravanan, M.; Ramesh, A. *Eur. J. Med. Chem.* **2001**, *36*, 615.
32. Manning, G.; Whyte, D. B.; Martinez, R.; Hunter, T.; Sudarsanam, S. *Science* **2002**, *298*, 1912.
33. Vieth, M.; Higgs, R. E.; Robertson, D. H.; Shapiro, M.; Gragg, E. A.; Hemmerle, H. *Biochim. Biophys. Acta* **2004**, *1697*, 243.
34. Lin, N. H.; Xia, P.; Kovar, P.; Park, C.; Chen, Z.; Zhang, H.; Rosenberg, S. H.; Sham, H. L. *Bioorg. Med. Chem. Lett.* **2006**, *16*, 421.
35. Jautelat, R.; Brumby, T.; Schafer, M.; Briem, H.; Eisenbrand, G.; Schwahn, S.; Kruger, M.; Lucking, U.; Prien, O.; Siemeister, G. *ChemBiochem* **2005**, *6*, 531.
36. Zhu, G. D.; Gandhi, V. B.; Gong, J.; Luo, Y.; Liu, X.; Shi, Y.; Guan, R.; Magnone, S. R.; Klinghofer, V.; Johnson, E. F.; Bouska, J.; Shoemaker, A.; Oleksijew, A.; Jarvis, K.; Park, C.; Jong, R. D.; Oltersdorf, T.; Li, Q.; Rosenberg, S. H.; Giranda, V. L. *Bioorg. Med. Chem. Lett.* **2006**, *16*, 3424.
37. Pike, A. C.; Rellos, P.; Niesen, F. H.; Turnbull, A.; Oliver, A. W.; Parker, S. A.; Turk, B. E.; Pearl, L. H.; Knapp, S. *EMBO J.* **2008**, *27*, 704.
38. Wernimont, K.; Artz, J. D.; Finerty, P., Jr.; Lin, Y. H.; Amani, M.; Allali-Hassani, A.; Senisterra, G.; Vedadi, M.; Tempel, W.; Mackenzie, F.; Chau, I.; Lourido, S.; Sibley, L. D.; Hui, R. *Nat. Struct. Mol. Biol.* **2010**, *17*, 596.
39. Rellos, P.; Ivins, F. J.; Baxter, J. E.; Pike, A.; Nott, T. J.; Parkinson, D. M.; Das, S.; Howell, S.; Fedorov, O.; Shen, Q. Y.; Fry, A. M.; Knapp, S.; Smerdon, S. J. *J. Biol. Chem.* **2007**, *282*, 6833.
40. Mologni, L.; Rostagno, R.; Brussolo, S.; Knowles, P. P.; Kjaer, S.; Murray-Rust, J.; Rosso, E.; Zambon, A.; Scapozza, L.; McDonald, N. Q.; Lucchini, V.; Gambacorti-Passerini, C. *Bioorg. Med. Chem.* **2010**, *18*, 1482.
41. Kutach, A. K.; Villasenor, A. G.; Lam, D.; Belunis, C.; Janson, C.; Lok, S.; Hong, L. N.; Liu, C. M.; Deval, J.; Novak, T. J.; Barnett, J. W.; Chu, W.; Shaw, D.; Kuglstatler, A. *Chem. Biol. Drug Des.* **2010**, *76*, 154.